Diagnosis of earth-fill dams by synthesised approach of sounding and surface wave method

Shin-ichi Nishimura, Toshifumi Shibata & Takayuki Shuku

Published online: 07 Jul 2016.

Submit your article to this journal ☐

View related articles ☐

View Crossmark data ☐

Taylor & Francis
Taylor & Francis Group

Diagnosis of earth-fill dams by synthesised approach of sounding and surface wave method

Shin-ichi Nishimura, Toshifumi Shibata and Takayuki Shuku

Graduate School of Environmental and Life Science, Okayama University, Okayama, Japan

ABSTRACT

The spatial distribution of the strength inside the earth-fill is identified by the sounding tests. In this research, the Swedish weight sounding (SWS) is employed, and the spatial high-density test is performed to identify the spatial correlation structure. Furthermore, the synthesised approach of the SWS and surface wave method, which is one of the geophysical method, is proposed to compensate the shortage of each approach. Consequently, the correlation structure of an earth-fill could be identified accurately, and the high resolution of the spatial distribution could be visualised based on the survey results.

1. Introduction

There are many earth-fill dams for irrigation in Japan. Some of them are getting old and decrepit and, therefore, have weakened. Making a diagnosis of the dams is important to increase the lifetime, and an investigation of the strength inside the embankment is required for this task. In the present research, the spatial distribution of the strength parameters of decrepit earth-fills is discussed, and an identification method for the distribution is proposed. Although the strength of the earth-fills is generally predicted from the standard penetration test (SPT) N-values, Swedish weight sounding (SWS) tests (e.g. JGS 2004) are employed in this research as a static sounding method of obtaining the spatial distribution of the N-values. The SWS test is advantageous in that they make short interval exams possible because of their simplicity.

In general, the identification of the spatial correlation of soil parameters is difficult, since the usual sampling intervals are greater than the spatial correlation. Therefore, sounding tests are convenient for determining the correlation lengths. Tang (1979) determined the spatial correlation of a ground by cone penetration tests (CPT). Cafaro and Cherubini (2002) also evaluated the spatial correlation with the CPT results. Uzielli, Vannucchi, and Phoon (2005) considered several types of correlation functions for the CPT results. Nishimura and Shimizu (2008) determined the correlation parameters of the N-value at the coastal dyke with the maximum likelihood method.

The information for the spatial correlation structures is important to perform the random field analysis. Fenton and Griffiths (2002), who analysed the settlement of the footing on the ground, considered the spatial correlation structure of Young's modulus. In addition, Griffiths, Fenton, and Manoharan (2002) calculated the bearing capacity by analysing the random field of the undrained shear strength using the elasto-plastic finite elements method. Nishimura, Murakami, and Matsuura (2010) applied the random field theory to the elasto-plastic model and evaluated the risk of the earth-fill dams.

The spatial distributions of the N-values can be identified based on the sounding tests with high resolution, since point estimations of the N-values are possible with short testing intervals. However, the predicted N-values are supposed to involve great prediction errors in parts for which no point estimated data are included. To compensate for this weak point, the surface wave method (SWM) (e.g. Hayashi 2004) is employed here, which is one of the geophysical exploration methods. By using this method, the shear wave (S-wave) distribution can be easily estimated as an averaged image over the wide area of an earth-fill, although the actual spatial fluctuations of the S-wave velocities are ignored throughout the inversion process. S-waves have a close correlation with the soil mechanical parameters, and are transformed into N-values in this research. Finally, two kinds of N-value distributions derived from sounding results and SWM are synthesised and then spatially

---

interpolated with the indicator simulation (Deutsch and Journel 1992).

2. Statistical model of *N*-values

A representative variable for the soil properties, s is defined by Equation (1) as a function of the location $\mathbf{X}$ = (x, y, z). Variable s is assumed to be expressed as the sum of the mean value m and the random variable U, which is a normal random variable in this study

$$s(\mathbf{X}) = m(\mathbf{X}) + U(\mathbf{X}). \quad (1)$$

The random variable function, $s(\mathbf{X})$, is discretised spatially into a random vector $\mathbf{s}^t = (s_1, s_2, \ldots, s_M)$, in which s_k is a point estimation value at the location $\mathbf{X} = (x_k, y_k, z_k)$. The soil parameters, which are obtained from the tests, are defined here as $\mathbf{S}^t = (S_1, S_2, \ldots, S_M)$. Symbol M signifies the number of test points. Vector $\mathbf{S}$ is considered as a realisation of the random vector $\mathbf{s}^t = (s_1, s_2, \ldots, s_M)$. If the variables $s_1, s_2, \ldots, s_M$ constitute the M-variate normal distribution, the probability density function of s can then be given by the following equation:

$$f_S(\mathbf{s}) = (2\pi)^{-M/2}|\mathbf{C}|^{-1/2}exp\{-\tfrac{1}{2}(\mathbf{s}-\mathbf{m})^t\mathbf{C}^{-1}(\mathbf{s}-\mathbf{m})\}, \quad (2)$$

in which $\mathbf{m}^t = (m_1, m_2, \ldots, m_M)$ is the mean vector of the random function $\mathbf{s}^t = (s_1, s_2, \ldots, s_M)$; and it is assumed to be following the regression function. In this research, a 2-D statistical model is considered, namely, the horizontal coordinate x, which is parallel to the embankment axis, and the vertical coordinate z are introduced here, while the other horizontal coordinate y, which is perpendicular to the embankment axis, is disregarded. The element of the mean vector is described as follows:

$$m_k = a_0 + a_1 x_k + a_2 z_k + a_3 x_k^2 + a_4 z_k^2 + a_5 x_k z_k, \quad (3)$$

in which (x_k, z_k) means the coordinate corresponding to the position of the parameter s_k, and a_0, a_1, a_2, a_3, a_4, and a_5 are the regression coefficients.

$\mathbf{C}$ is the $M \times M$ covariance matrix, which is selected from the following four types in this study:

$$\mathbf{C} = [C_{ij}] =$$

$$\sigma^2 \exp\left(-(x_i - x_j)/l_x - (z_i - z_j)/l_z\right), \quad (4a)$$

$$\sigma^2 \exp\{-(x_i - x_j)^2/l_x^2 - (z_i - z_j)^2/l_z^2\}, \quad (4b)$$

$$\sigma^2 \exp\left\{-\sqrt{(x_i - x_j)^2/l_x^2 + (z_i - z_j)^2/l_z^2}\right\}, \quad (4c)$$

$$N_e\sigma^2 \exp\left(-(x_i - x_j)/l_x - (z_i - z_j)/l_z\right), \quad (4d)$$

$$i, j = 1, 2, \ldots, M$$

$$N_e = 1 \quad (i = j)$$
$$N_e \leq 1 \quad (i \neq j),$$

in which the symbol $[C_{ij}]$ signifies an i–j component of the covariance matrix, σ is the standard deviation, and l_x and l_z are the correlation lengths for the x and z directions, respectively. Parameter N_e is related to the nugget effect. The Akaike's Information Criterion, AIC (Akaike 1974), is defined by Equation (5), considering the logarithmic likelihood

$$\text{AIC} = -2 \cdot \max\{\ln f_S(\mathbf{S})\} + 2L = M \ln 2\pi$$
$$+ \min\{\ln|\mathbf{C}| + (\mathbf{S}-\mathbf{m})^t\mathbf{C}^{-1}(\mathbf{S}-\mathbf{m})\} + 2L, \quad (5)$$

in which L is the number of unknown parameters included in Equation (2). By minimising AIC (MAIC), the regression coefficients of the mean function, the number of regression coefficients, the standard deviation, σ, a type of the covariance function, the nugget effect parameter, and the correlation lengths are determined.

Because the correlation lengths of soil parameters are often short compared with the sampling or the testing interval, sometimes the correlation lengths cannot be determined using the aforementioned method. For such cases, the following two-step approach is proposed as a strategy for identifying the spatial correlation structure. First, the mean (trend) function and the variances are determined by MAIC. Subsequently, the covariance C_{ij} is determined from the semi-variogram. The semi-variogram is evaluated in the horizontal and vertical directions as individual functions of the sampling intervals

$$\gamma_x(q \cdot \Delta x) = \frac{\sum_{j=1}^{N_z}\sum_{i=1}^{N_x-q}\{U(x_i, z_j) - U(x_i + q\cdot\Delta x, z_j)\}^2}{2N_z(N_x - q)},$$

$$\gamma_z(q \cdot \Delta z) = \frac{\sum_{j=1}^{N_x}\sum_{i=1}^{N_z-q}\{U(x_j, z_i) - U(x_j, z_i + q\cdot\Delta z)\}^2}{2N_x(N_z - q)},$$

$$q = 1, 2, \ldots \quad (6)$$

where γ_x, and γ_z are the semi-variaograms for the x, and the z directions, respectively, $U(x,z)$ is a measured parameter at the point (x,z) from which the mean value is removed, namely, the value of $(s(x,z)-m(x,z))/\sigma$, Δx and Δz are sampling intervals, and N_x and N_z are the number of sampling points for the x and the z directions, respectively. Next, the calculated semi-variograms are approximated by the following theoretical semi-variogram functions, and the correlation lengths are identified. Since an exponential type of function (Equation

(4a)) is selected as the best fitting function by MAIC in many cases, it is also employed here

$$\gamma_x(|x_i - x_j|) = C_{0x} + C_{1x}\{1 - \exp(-|x_i - x_j|/l_x)\} \, i \neq j,$$
$$\gamma_z(|z_i - z_j|) = C_{0z} + C_{1z}\{1 - \exp(-|z_i - z_j|/l_z)\} \, i \neq j,$$
$$\gamma_x(0) = \gamma_z(0) = 0.$$

(7)

In Equation (7), C_{0x} and C_{0z} are the parameters used for the nugget effect for the x and the z directions, respectively, and C_{1x}, and C_{1z} are the parameters used to express the shape of the semi-variogram functions.

Finally, the two-dimensional covariance C_{ij} between two points i and j, is given as

$$C_{ij} = \sigma^2 C_{1x} C_{1z} \exp\left(-\frac{|x_i - x_j|}{l_x} - \frac{|z_i - z_j|}{l_z}\right), \quad i \neq j$$
$$C_{ij} = \sigma^2, \quad i = j.$$

(8)

3. Indicator simulation method

The N-value is estimated based on the two kinds of data. One is the sounding test and the other is the SWM, a kind of elastic wave survey method. Surface waves are strongly related to shear waves, and are easily related to the N-values. These two sets of results are conveniently synthesised with the indicator simulation method, a kind of geostatistical method, which can simultaneously treat hard data (primary data) and soft data (secondary data). Herein, the SWS results are considered as the hard data, while the surface wave results are the soft data.

An indicator value, i, for a parameter, R is expressed by

$$i(\mathbf{u}; r_k) = \begin{cases} 1, & (R(\mathbf{u}) \leq r_k), \\ 0, & (R(\mathbf{u}) > r_k), \end{cases} \quad k = 1, \ldots, K, \quad (9)$$

in which the vector $\mathbf{u} = (x, z)$ means the positions where the data were measured, and the parameter R is given as a function of $\mathbf{u}$. The values of r_k ($k = 1, 2, \ldots, K$) are K specific values of R, and the threshold value for the binary parameter i. The probability distribution function of the variable R, F is defined in the following:

$$F(\mathbf{u}; r_k((n + n'))) = \text{Prob}\{R(\mathbf{u}) \leq r_k((n + n')\}$$

$$= \lambda_0 F(r_k) + \sum_{\alpha=1}^{n} \lambda_\alpha(\mathbf{u}; r_k) i(\mathbf{u}_\alpha; r_k)$$

$$+ \sum_{\alpha'=1}^{n'} \nu_{\alpha'}(\mathbf{u}; r_k) w(\mathbf{u}_{\alpha'}; r_k),$$

(10)

$$\lambda_0 = 1 - \sum_{\alpha=1}^{n} \lambda_\alpha(\mathbf{u}; r_k) - \sum_{\alpha'=1}^{n'} \nu_{\alpha'}(\mathbf{u}; r_k),$$

where $i(\mathbf{u}_\alpha; r_k)$ means the binary value of the hard data at the point $\mathbf{u}_\alpha$, and for the threshold value r_k, $w(\mathbf{u}_{\alpha'}; r_k)$ is the soft data, and n and n' are the numbers of the hard and the soft data, respectively. The parameters λ and ν are the weighting parameters corresponding to the arbitrary point $\mathbf{u}m$ for the interpolation; they are determined by solving following equation:

$$\sum_{\beta=1}^{n} \lambda_\beta(\mathbf{u}_m; r_k) C_{\beta\alpha} + \sum_{\beta'=1}^{n'} \nu_{\beta'}(\mathbf{u}_m; r_k) C_{\beta'\alpha} = C_{m\alpha},$$

$$\alpha = 1, \ldots, n,$$

$$\sum_{\beta=1}^{n} \lambda_\beta(\mathbf{u}_m; r_k) C_{\beta\alpha'} + \sum_{\beta'=1}^{n'} \nu_{\beta'}(\mathbf{u}_m; r_k) C_{\beta'\alpha'} = C_{m\alpha'},$$

$$\alpha' = 1, \ldots, n',$$

(11)

in which $C_{\beta\alpha}$, $C_{\beta'\alpha'}$, $C_{m\alpha}$, and $C_{m\alpha'}$ are the covariance matrices between two points, namely, $(\mathbf{u}_\beta, \mathbf{u}_\alpha)$, $(\mathbf{u}_{\beta'}, \mathbf{u}_{\alpha'})$, $(\mathbf{u}_m, \mathbf{u}_\alpha)$, and $(\mathbf{u}_m, \mathbf{u}_{\alpha'})$, respectively. The soft data w are derived from the following process based on the indicator kriging (Deutsch and Journel 1992).

(1) The measured data from the surface wave test results are assigned for the points α's on the space as the input data for the indicator kriging.
(2) The probability distribution function $F(r_k)$ of the SWS results is assumed for the measured data.
(3) Indicator kriging is conducted based on the measured SWM data and the probability distribution function $F(r_k)$.
(4) The results of the indicator kriging, which are presented by the probability distributions at the n' points, are employed as the soft data in the indicator simulation.

Based on the probability distribution function $F(\mathbf{u}; r_k| n + n')$ updated by the soft data, the random numbers are created from the following equation:

$$r^{(l)}(\mathbf{u}) = F^{-1}(\mathbf{u}; p^{(l)}((n + n')),$$

(12)

where p is the uniform random number from 0 to 1.0, and l is the iteration number for the Monte Carlo method. Finally, a random number, $r^{(l)}$, is assigned to the N-value.
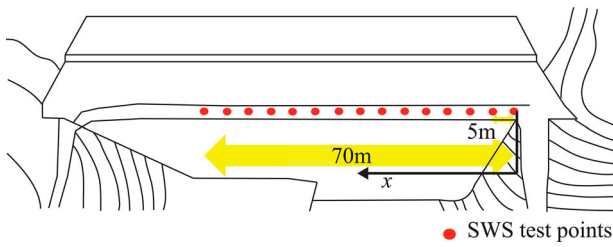
Figure 1. Plan view of embankment and testing interval.

4. SWS and SWM results and geostatistical analyses

4.1. In situ *test results*

Although high-density sampling is required in order to evaluate the spatial distribution of soil parameters, the amount of data is not sufficient in the general sampling plans. In such cases, sounding is a convenient way to identify the spatial distribution structure of the soil parameters. In this research, an embankment at Site A is analysed, for which SWS tests were conducted at 15 points, at 5 m intervals, along the embankment axis, as shown in Figure 1. Additional tests were conducted between $x = 18$ m and $x = 24$ m with 2 m interval to identify the lateral correlation length. The soil profile for the embankment is presented with cross section in Figure 2, and it is categorised as intermediate soil, and consists of the decomposed granite.

Generally, the strength parameters are assumed based on SPTs with the use of empirical relationships. In this research, however, SWS tests, which are simpler than SPT, are employed instead of SPT. Inada (1960) derived the relationship between the results of SPT and SWS. Equation (13) shows the relationship for sandy grounds, while Figure 3 shows the relationship between SWS and SPT *N*-values.

$$N_{SWS} = 0.002 W_{SW} + 0.67 N_{SW}, \quad (13)$$

in which N_{SWS} is the N-value derived from SWS, N_{SW} is the number of half rations and W_{SW} is the total weight of the loads (unit: N). Based on these data, the variability of the relationship is evaluated in this study, and the
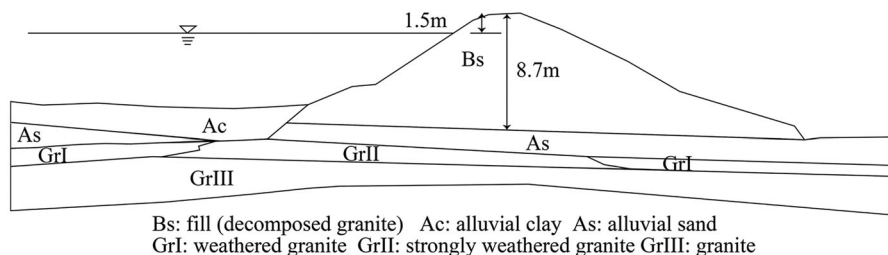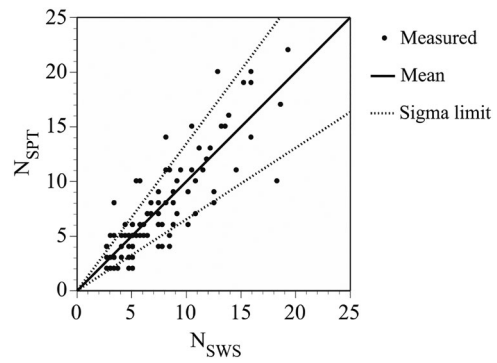

Figure 3. Relationship between SWS results and SPT *N*-values (Nishimura, Shuku, and Shibata 2014).

coefficient of variation is determined as 0.354. The value of 0.354 can be derived as the standard deviation of the measured N_{SPT}/N_{SWS} values. The determined σ-limits, which are the values apart from the mean value with the standard deviation, are also shown in Figure 3 with broken lines. Considering the variability of the relationship, the SPT N-value, N_{SPT} is modelled by

$$N_{SPT} = (1 + 0.354\varepsilon_r)N_{SWS}, \quad (14)$$

in which ε_r is an $N(0,1)$ random variable (Nishimura, Shuku, and Shibata 2014).

In Figure 4, the distribution of the N-values predicted by the SWM is exhibited. The figure shows the averaged image throughout the inversion. Equation (15) is employed to transform the measured shear wave, V_s, to
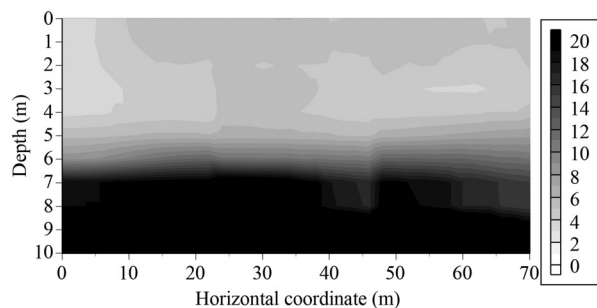

Figure 4. *N*-value distribution by SWM.

Bs: fill (decomposed granite)   Ac: alluvial clay   As: alluvial sand
GrI: weathered granite   GrII: strongly weathered granite   GrIII: granite

Figure 2. Cross section of an embankment and soil profiles.

the N-value (Imai, Fumoto, and Yokota 1975)

$$V_S = 97.0N^{0.314}. \tag{15}$$

Surface waves are closely correlated to shear waves V_s, which in turn have a strong correlation to the elastic modulus and the N-values. In this research, the surface wave was measured as 70 m along the embankment axis at 2 m intervals.

4.2. Statistical mode

The mean function and the covariance function of the SWS N-value, N_{SWS}, are determined with MAIC, and the mean is exhibited in Figure 5. The mean and the covariance functions given by Equations (3) and (4) were examined, and the optimum functions are determined as Equations (16) and (17). The horizontal correlation length l_x is identified as being approximately 10 m, and the vertical one, l_z, is 2.66 m. Compared with the published values (Tang 1979; DeGroot and Beacher 1993; Phoon and Kulhawy 1999; Nishimura, Murakami, and Matsuura 2010), the horizontal one is reasonable, and vertical one is rather large. The horizontal length, however, is almost three times of the vertical one, and the values could be acceptable due to the fact that the horizontal length is much greater than the vertical one

$$m = 2.52 - 0.0279x - 0.226z + 0.0003x^2$$
$$+ 0.0465z^2 + 0.0038xz, \tag{16}$$

$$[C_{ij}] = N_e\sigma^2 \exp(-\Delta x_i/l_x - \Delta z_i/l_z),$$
$$\begin{cases} N_e = 1 & (i = j), \\ N_e = 0.73 & (i \neq j), \end{cases} \tag{17}$$

$$\sigma = 1.08, \quad l_x = 9.88\text{m}, \quad l_z = 2.66\text{m}.$$

To check the correlation structures, the semi-variograms for the horizontal and vertical directions are calculated. Figure 6(a) and 6(b) shows the semi-variograms for the lateral and vertical directions, respectively.
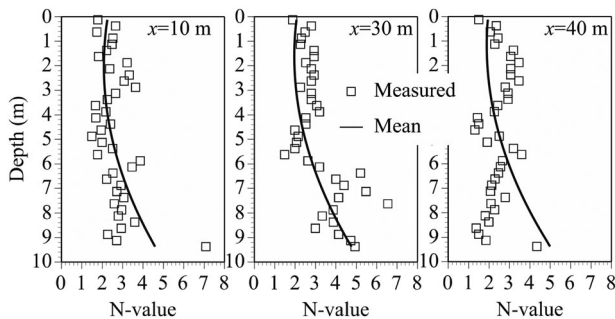
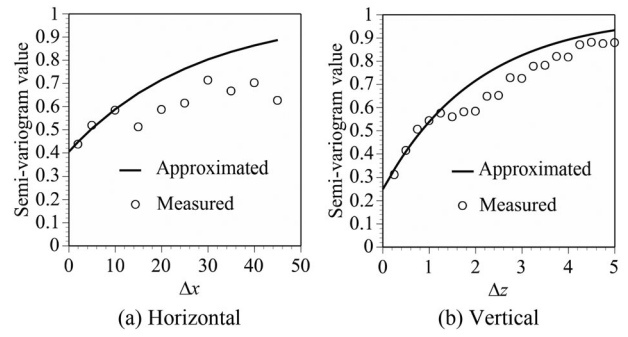**Figure 5.** Distributions of the SWS N-value.

Figure 6. Semi-variograms and approximate functions. (a) Horizontal and (b) vertical.

The semi-variogram values of $\Delta x = 2$, 5, and 10 m, $\Delta z = 0.25$, 0.5, 0.75, 1.0, 1.25 m are employed to identify the approximate functions of Equation (7) for the lateral and vertical directions. Since the values of N_x and N_z in Equation (6) are large within the short intervals of Δx and Δz, the accuracy of the semi-variogram values is supposed to be high. The result is exhibited as follows:

$$C_{x1} \cdot C_{z1} = 0.45, \quad l_x = 27.1 \text{ m}, \quad l_z = 2.06 \text{ m}.$$

The value of the nugget effect for the lateral direction, 0.4, seems very large. The reason is as follows. To identify the lateral correlation, the semi-variogram values are calculated from the data obtained in the same depth. Since the variability of the measured data along the depth of each test point is great as shown in Figure 4, the calculated lateral correlation can be easily affected by the variability, and in the results, the lateral semi-variogram can include uncertainty as the nugget effect.

The lateral correlation length is identified as almost three times of the MAIC, while the vertical length is determined as the value similar to that of the MAIC. There is a tendency generally that the variogram exhibits relatively longer correlation length, compared with the MAIC, since the correlation lengths l_x and l_z are identified separately along the single coordinate of x or z with selected intervals, Δx, and Δz, which exhibit high correlations in the calculation of the variogram. While in the MAIC, the multi-dimensional normal distribution is assumed, the correlation structures of obtained data in all test points must be identified simultaneously.

4.3. Synthesis of SWS and SWM results

The SWS are the actual destruction tests, and they can estimate accurate N-values with high resolution as point estimated values. The accuracy of the measured values at the measuring points is good, while at the mid-points between two measuring points, the accuracy

is inferior to that at the measuring points. While the SWM is convenient for obtaining the averaged profile, the local resolution is not good. If the results of the two methods are synthesised, the shortcoming of one method can be compensated by the other method. In this research, the results for SWS and SWM are considered as the hard and the soft data, respectively, and then the two sets of results are synthesised with the indicator simulation method.

As for the mean and the covariance functions, Equations (16) and (17) are employed for the embankment. In the Monte Carlo simulation, random numbers for N_{SWS} are generated through Equation (12). Then random numbers for N_{SPT} are created by considering error factor ε_R in Equation (14). The spatial statistical values for N_{SPT} are discussed below.

Figures 7 and 8 present the analytical cases without and with the soft data, respectively. Figures (a), (b), and (c) correspond to the mean, the standard deviation, and the probability that N- value falls below 2, respectively.

According to Figure 7(a), around depth $z = 3–4$ m, $x = 30–40$ m, the lowest value is detected. Corresponding to Figure 6(a), the lowest value of probability is obtained at the same location in Figure 7(c). In Figure 8(a), the left part of the embankment shows a lower value, compared with Figure 7(a), and corresponding to this result, the probability is relatively high in the left side as depicted in Figure 8(c). The deeper part of the embankment, $z = 7–9$ m, the high average of N-value and smaller probability are exhibited in Figure 8(a) and 8(c) due to the fact the SWM results are affected by the base ground. Comparing Figures 7(b) and 8(b), the standard deviation

(a) Mean (N-Value)

(b) Standard deviation (N-Value)
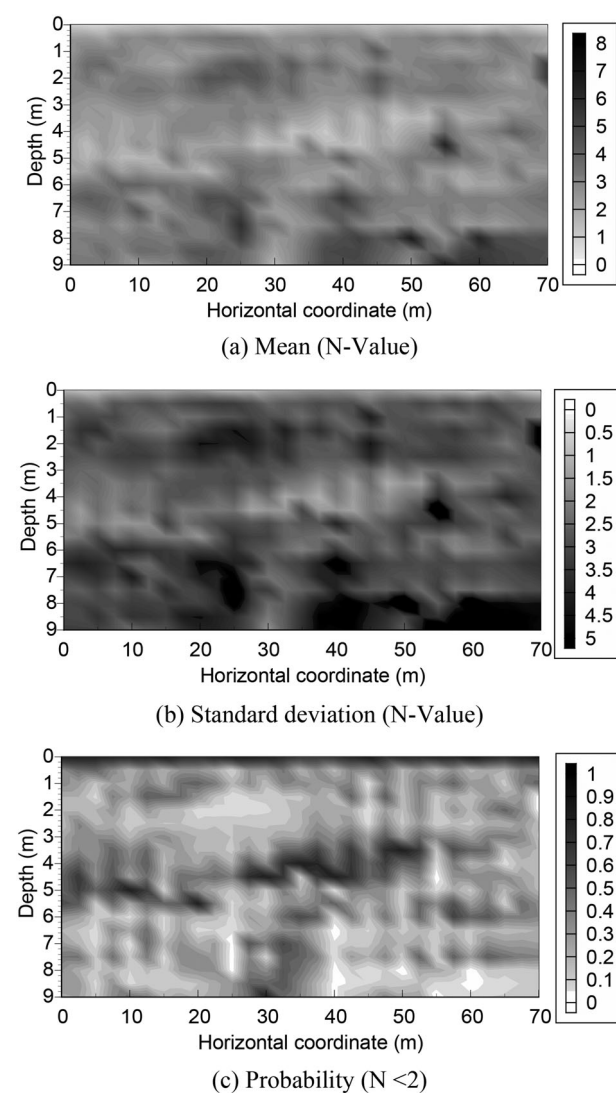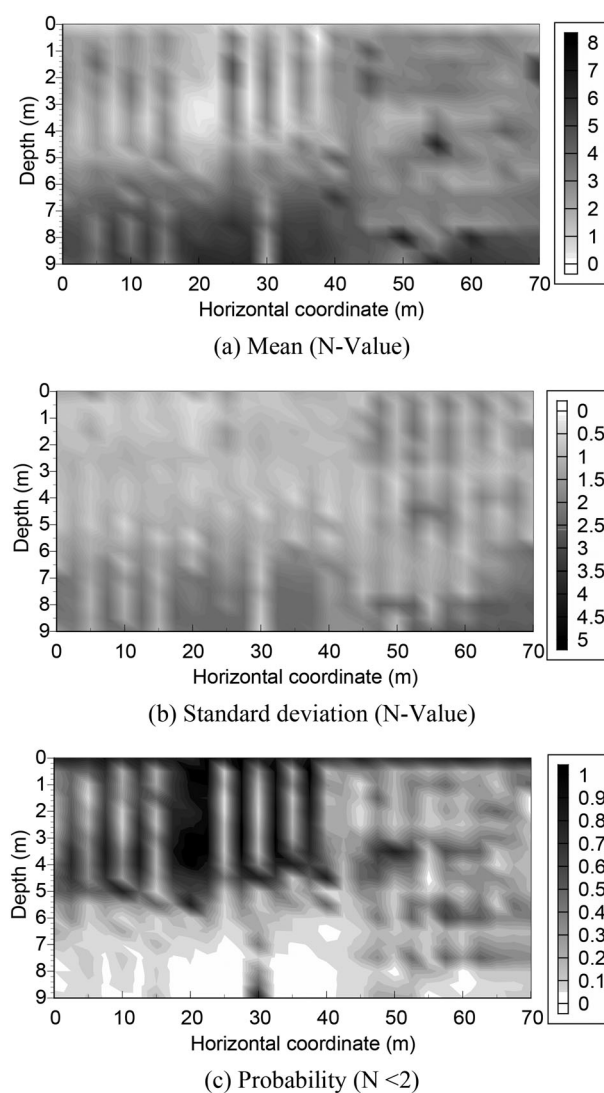
(c) Probability (N <2)

Figure 7. Statistical values of *N*-value by indicator simulation without soft data. (a) Mean (*N*-value), (b) standard deviation (*N*-value), and (c) probability (*N* < 2).

(a) Mean (N-Value)

(b) Standard deviation (N-Value)

(c) Probability (N <2)

Figure 8. Statistical values of *N*-value by indicator simulation with soft data. (a) Mean (*N*-value), (b) standard deviation (*N*-value), and (c) probability (*N* < 2).
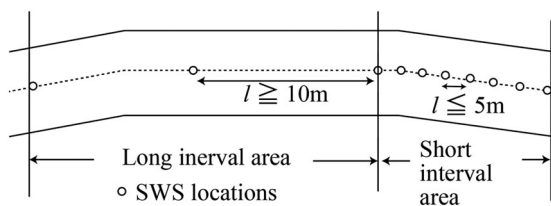
Figure 9. Test procedure of SWS and SWM.

in the latter case is smaller than the former case, and it is understood that the uncertainty of the N-values can be reduced with the soft data.

According to the comparison between Figures 7(c) and 8(c), safety side results are obtained with the synthesis of the results of the SWS and SWM in the studied case, since greater probability is obtained inside the embankment in Figure 8(c).

4.4. Practical procedure of SWS and SWM

The strategy of practical use for the synthesis of SWS and SWM is presented here. Figure 9 describes the plan view of tested embankment. The SWM should be conducted in the whole tested area, since it is an economical and efficient method. Although the SWS tests should be conducted also in the whole area to identify the accurate strength distributions, the long interval and short intervals of the SWS should be mixed. The former is employed for the efficiency of testing, in which the SWM results work dominantly, the latter is important to identify the spatial correlations of the strength parameter.

5. Conclusions

(1) With minimum lateral interval of SWS of 2 m, the spatial correlation structures of N-values inside the embankment could be evaluated accurately.
(2) Correlation structures were obtained by two approaches, MAIC and semi-variogram, and the difference of two results was acceptable.
(3) The spatial distribution of the probability that the N-value is lower than the threshold value has been calculated with the indicator simulation. The spatial distribution of the probability can be used for the health monitoring of the inside of an embankment.
(4) As an application of this work, the distribution of the N-values is used for the reliability analysis of the embankments, and then the N-values are transformed to the strength parameters such as the internal friction angles. In the transformation, the uncertainty of the relationship between the N-values and the strength

parameters must be evaluated as a transformation error. The transformation error can be a dominant factor for the calculated probability of failure.

References

Akaike, H. 1974. "A New Look at the Statistical Model Identification." *IEEE Transactions on Automatic Control* 19 (6): 716–723.

Cafaro, F., and C. Cherubini. 2002. "Large Sample Spacing in Evaluation of Vertical Strength Variability of Clayey Soil." *Journal of Geotechnical and Geoenvironmental Engineering* 128 (7): 558–568.

DeGroot, D. J., and G. B. Beacher. 1993. "Estimating Autocovariance of In-situ Soft Properties." *Journal of the Geotechnical Engineering* 119 (1): 147–166. ASCE.

Deutsch, C. V., and A. G. Journel. 1992. *Geostatistical Software Library and User's Guide*. New York: Oxford University Press.

Fenton, G. A., and D. V. Griffiths. 2002. "Probabilistic Foundation Settlement on Spatial Random Soil." *Journal of Geotechnical and Geoenvironmental Engineering* 128 (5): 381–391.

Griffiths, D. V., G. A. Fenton, and N. Manoharan. 2002. "Bearing Capacity of Rough Rigid Strip Footing on Cohesive Soil: Probabilistic Study." *Journal of Geotechnical and Geoenvironmental Engineering* 128 (9): 743–755.

Hayashi, K. 2004. "Estimation of Near-Surface Shear Wave Velocity Model Using Surface –Waves." *Journal of JSNDI* 53 (5): 254–259.

Imai, T., H. Fumoto, and K. Yokota. 1975. Velocity of Elastic Wave and Mechanical Properties in Japanese Grounds, Paper presented at the proceedings of 4th symposium of Earthquake Engineering, 89–96 (in Japanese).

Inada, M. 1960. "Usage of Swedish Weight Sounding Results." *Geotechnical Engineering Magazine* 8 (1): 13–18 (in Japanese).

Japanese Geotechnical Society. 2004. *Japanese Standards for Geotechnical and Geoenvironmental Investigation Methods – Standards and Explanations-*. Tokyo: JGS. (in Japanese).

Nishimura, S., A. Murakami, and K. Matsuura. 2010. "Reliability-Based Design of Earth-Fill Dams Based on the Spatial Distribution of Strength Parameters." *Georisk* 4 (3): 140–147.

Nishimura, S., and H. Shimizu. 2008. "Reliability-Based Design of Ground Improvement for Liquefaction Mitigation." *Structural Safety* 30: 200–216.

Nishimura, S., T. Shuku, and T. Shibata. 2014. "Reliability-Based Design of Earth-Fill Dams to Mitigate Damage Due

to Severe Earthquakes, Vulnerability, Uncertainty and Risk." Paper presented at the proceedings of 2nd ICVRAM – 6th ISUMA, July 13–16, 2350–2359.

Phoon, K-K. and F. H. Kulhawy. 1999. "Evaluation of Geotechnical Property Variability." *Canadian Geotechnical Journal* 36: 625–639.

Tang, W. H. 1979. "Probabilistic Evaluation Penetration Resistances." *Journal of the Geotechnical Engineering* 105 (GT10): 1173–1191. ASCE.

Uzielli, M., G. Vannucchi, and K. K. Phoon. 2005. "Random Field Characterization of Stress-Normalized Cone Penetration Testing Parameters." *Geotechnique* 55 (1): 3–20.